Millennial-scale precipitation variability over Easter Island (South Pacific) during MIS 3: Inter-hemispheric teleconnections with North Atlantic abrupt cold events

O. Margalef [1], I. Cacho [2], S. Pla-Rabes [1], N. Cañellas-Boltà [3], J. J. Pueyo [2], A. Sáez [2], L. D. Pena [2], B. L. Valero-Garcés [4], V. Rull [3], S. Giralt [3]

[1]{ Ecological Research Center and Forestry Applications (CREAF). Campus de Bellaterra (UAB) E-08193 Cerdanyola del Vallès, Barcelona. Spain. }

[2]{ Faculty of Geology, Universitat de Barcelona, Martí Franquès s/n, E-08028 Barcelona, Spain}

[3]{ Institute of Earth Sciences Jaume Almera (ICTJA-CSIC), Sedimentary Geology and Geohazards, Lluís Solé i Sabarís s/n, E-08028 Barcelona, Spain.}

[4]{Pyrenean Institute of Ecology (IPE-CSIC). Avda. de Montañana 1005, E-50059 Zaragoza, Spain.}

Correspondence to: Olga Margalef (omargalefgeo@gmail.com)

Abstract

Marine Isotope Stage 3 (MIS 3, 59.4-27.8 kyr BP) is characterized by the occurrence of rapid millennial-scale climate oscillations known as Dansgaard-Oeschger cycles (DO) and by abrupt cooling events in the North Atlantic known as Heinrich events. Although both the timing and dynamics of these events have been broadly explored in North Atlantic records, the response of the tropical and subtropical latitudes to these rapid climatic excursions, particularly in the Southern Hemisphere, still remains unclear. The Rano Aroi peat record (Easter Island, 27ºS) provides a unique opportunity to understand atmospheric and oceanic changes in the South Pacific during these DO cycles because of its singular location, which is influenced by the South Pacific Anticyclone (SPA), the Southern Westerlies (SW), and the Intertropical Convergence Zone (ITCZ) linked to the South Pacific Convergence Zone (SPCZ). The Rano Aroi sequence records 6 major events of enhanced precipitation between 38 and 65 kyr BP. These events are compared with other hydrological records from the tropical and subtropical band supporting a coherent regional picture, with the dominance of humid conditions in Southern Hemisphere tropical band during Heinrich Stadials (HS) 5, 5a and 6 and other Stadials while dry conditions prevailed in the Northern tropics. This antiphased hydrological pattern between hemispheres has been attributed to ITCZ migration, which in turn might be associated with an eastward expansion of the SPCZ storm track, leading to an increased intensity of cyclogenic storms reaching Easter Island. Low Pacific Sea Surface Temperature (SST) gradients across the Equator were coincident with the here-defined Rano Aroi humid events and consistent with a reorganization of Southern Pacific atmospheric and oceanic circulation also at higher latitudes during Heinrich and Dansgaard-Oeschger stadials.

1 Introduction

On suborbital timescales, climate in the Northern Hemisphere during MIS 3 was dominated by rapid millennial-scale temperature oscillations defined as the Dansgaard-Oeschger (DO) stadial-interstadial cycles (Dansgaard et al., 1993). During some of the DO stadials, large *armadas* of icebergs covered the North Atlantic Ocean, causing the so-called Heinrich events, which induced a rapid weakening of the Atlantic Meridional Overturning Circulation (AMOC) (Heinrich, 1988; Broecker, 1994; Ganopolski and Rahmstorf, 2002 Hemming, 2004).

Although most of the records documenting this rapid climate variability are concentrated in the North Atlantic region, a number of studies from the tropical Atlantic and Pacific Oceans point towards a linkage between cooling episodes in the North Atlantic records and millennial-scale changes in Sea Surface Temperature (SST), humidity and marine productivity in the tropics (Baker et al., 2001; Haug et al, 2001; Wang et al., 2004, 2007; Muller, 2006; Clement and Peterson, 2008). This evidence suggests a connection between high and low latitudes to rapid climatic oscillations during last glacial cycle, which likely involved a tied ocean-atmosphere coupling (Oppo et al., 2003). Some tropical and subtropical records of MIS 3 from Africa, South America and Australia show changes in precipitation patterns during Heinrich Stadials (HS) (Wang et al., 2004; Muller, 2006; Tierney et al., 2008). MIS 3 changes in SST and salinity in the West Equatorial Pacific have been interpreted as changes in the super El Niño-Southern Oscillation (ENSO) state (Stott et al., 2002), whereas others have regarded changes in tropical rainfall as evidence of latitudinal displacements of the Intertropical Convergence Zone (ITCZ) (Wang et al, 2007; Leduc et al., 2009).

Currently, there are few records available with an appropriate temporal resolution to characterize millennial-scale changes in tropical and subtropical areas (Arz et al., 1998; Peterson et al., 2000; Rosenthal et al., 2000; Haug et al., 2001; Wang et al., 2004; Cruz et al, 2005; Muller et al., 2006; Wang et al., 2007; Conroy et al., 2008). However, none of these records is adequate for tracking changes over Central Pacific, an area were paleoceanographical records are absent due to the extremely low marine primary productivity which makes the sediments unsuitable for such climatic reconstructions. Easter Island is situated in a key area for understanding South Pacific climate, filling a regional gap without proper paleoclimatic registers suitable to understand MIS 3 climate. The Rano Aroi peatland is located in the highest area of Easter Island and its environmental history and has been extensively studied from an interdisciplinary approach (Margalef et al., 2013; Margalef et al., 2014). The hydroclimatic sensitivity of this mire, the broad multiproxy dataset available and the adequate resolution of its record makes Rano Aroi an excellent location to provide a comprehensive reconstruction of the South Pacific Convergence Zone (SPCZ) evolution during the MIS 3.

In order to better understand the regional ocean-atmosphere connections, the Rano Aroi record dataset (Margalef et al., 2013; Margalef et al., 2014) is compared to a new suite of equatorial SST gradient estimations based on previously published SST reconstructions. For the very first time a Late Pleistocene record from Central Pacific is compared with precipitation patterns on Southern Hemisphere tropics and the changes in atmospheric and oceanic circulation. We also compare the Rano Aroi record to high latitude datasets from the Northern and Southern Hemispheres to discuss the inter-latitudinal connections responsible for the propagation of rapid climate variability during MIS 3. The role of high latitude dynamics over the tropical paleoclimate and the inverse effect has been a matter of intense debate and increasing interest (Skinner et al., 2010). Inter-hemispheric and latitudinal tele-connections are new challenging frontiers for paleoclimatology.

2 Study site

Easter Island (Chile, 27º 07'S, 109º 22'W), or Rapa Nui in the local indigenous language, is a small Miocene volcanic island in the South Pacific Ocean, 3510 km from the South American continent (Table 1). The climate at the study site is subtropical, with average monthly temperatures oscillating between 18 and 24°C and with a highly variable annual rainfall (mean value 1130 mm) (Junk and Claussen, 2011).

The climate on Easter Island displays low seasonality. However, a seasonal latitudinal migration of the ITCZ, SPCZ and westerly storm track is responsible for higher precipitation rates between March and June. Two processes are responsible for rainfall formation over Easter Island: (1) cyclonic storms associated with SPCZ dynamics and pushed eastwards by the Southern Westerlies (Sáez et al., 2009, Junk and Claussen, 2011), and (2) land-sea breeze convection storms (Junk and Claussen, 2011). An analysis of the 1987-2005 satellite data performed within the framework of the HOAPS-3 project indicates that Easter Island lies at the active edge of the SPCZ, with associated precipitation rates between 657 and 803 mm/y (Andersson et al., 2007, Junk and Claussen, 2011). This analysis of the HOAPS-3 dataset excluded topographic effects, and for this reason, the disparity between estimated and recorded rainfall rates has been attributed to the contribution of island topography to convective storms (Junk and Claussen, 2011).

Paleoenvironmental studies from Easter Island have traditionally been based on pollen analyses (Flenley and King, 1984; Flenley et al., 1991; Dumont et al., 1998; Butler et al., 2004; Gossen, 2007; Azizi and Flenley, 2008; Horrocks and Wozniak, 2008; Mann et al., 2008, Cañellas-Boltà et al. 2013) and macrofossils remains (Dumont et al., 1998; Orliac and Orliac, 1998; Orliac, 2000; Peteet et al., 2003; Mann et al., 2008; Cañellas-Boltà et al., 2012), which have allowed the reconstruction of regional paleoclimatic and paleoenvironmental conditions from the last glacial period to the Holocene (Flenley et al., 1991; Azizi and Flenley 2008; Rull et al., 2010a). Recent multiproxy studies which combined sedimentological, mineralogical, geochemical and biological data, have also documented hydrological changes in Easter Island since ca. 34 kyr cal BP (Sáez et al., 2009; Cañellas-Boltà et al., 2012; Cañellas-Boltà et al., 2013) and since MIS 4 (Margalef et al., 2013).

The Rano Aroi mire (27° 5' 36"S - 109º 22' 25"W, 430 m elevation) is located in a volcano crater near the highest summit of the island, Mauna Terevaka (511 m asl). The chemical composition of the flowing Rano Aroi outlet (lightly acidic, pH=5.5-6.5) is similar to that of the region's groundwater. Water isotopic data ($\delta^{18}O$ and $\delta^{2}H$) indicates that waters are renewed through discharge from an aquitard, which is quite sensitive to seasonal variations in precipitation (Herrera and Custodio, 2008). The hydrology configuration in this region indicates that Rano Aroi is a self-sealing mire fed by deeper discharging groundwater rather than by interflow (Margalef et al., 2013).

3 Methodology

Precise information about field campaign, peat sampling and chemical analyses (TC, TN, $\delta^{13}C$, Fe, Ti and Ca) can be found in Margalef et al., (2013). $\delta^{13}C$ variability ($\delta^{13}C_{res}$) was analyzed by subtracting a 19-sample mean running average from the raw $\delta^{13}C$ data to highlight high-frequency events compared to long-term tendencies. This 6-variables dataset was selected because it permits to reconstruct the main environmental processes controlling Rano Aroi geochemical evolution (Margalef et al., 2013).

Detailed explanations on age model construction can be found in *Additional information* and Margalef et al. (2013). Chronologic uncertainties are one of the most common troubles on studies comprising the MIS 3 period, because they are situated beyond the radiocarbon limit (Russell et al., 2014). In this study we estimate age-depth relationship using a mixed-effect model and constant variance (Heegaard et al., 2005) using R software (R Development Core

Team, 2011). This method highlights not only the error estimate of the sample, but also the uncertainty related to how representative the obtained age is in relation to the object level. The procedure combines two random effects (within-object variance and between-object variance) obtaining better confidence intervals than other methodologies for modeling ages beyond the dating limit (Heegaard et al., 2005). This mixed regression method has been run to model the age-depth relation in the well constrained part of the record (235-750 cm depth). The obtained model was used to determine the age of the bottommost part of the register (750-1100cm), older than the radiocarbon dating limit.

Statistical treatment of the data was performed with R software (R Development Core Team, 2011) and the 'vegan' package (Oksanen et al., 2005). Principal component analysis (PCA) on the data that represented the MIS 3 was run to extract the main components of variability of the geochemical data (TC, TN, $\delta^{13}C_{res}$, Fe, Ti and Ca), standardizing and omitting samples with missing values. As in Margalef et al. (2013) and because of the different sampling resolution of the XRF dataset (2 mm) and of the geochemical data (5 cm), the XRF dataset was resampled at 5 cm intervals to make both datasets comparable. The resampling involved obtaining the mean values of the Ca, Ti and Fe measurements in every 5 cm.

A new gradient estimation between the Western and Eastern Equatorial Pacific have been calculated using previously published SST datasets from sites ODP 1240 site in the Eastern Equatorial Pacific Ocean (Pena et al., 2008) and core MD97-2141 in the Western Pacific Ocean (Table 1, Dannenmann et al., 2003). The temperature calibrations were those used by authors in their original publications and have been interpreted to reflect mostly annual average temperature (Dannenmann et al., 2003; Pena et al., 2008). Previously to the calculation, all the SST records were resampled at common age interval (every 250 years) using R software (R Development Core Team, 2011). For an extended explanation of the criteria followed to choose these sites to construct the gradient see *Additional information*.

4 Results

4.1 Geochemistry and peat facies

According to Margalef et al. (2013, 2014), the Rano Aroi sequence ARO 06 01 is composed of radicel peat sensu Succow and Joosten (2001). Four facies have been defined based on plant components, chemical composition, grain size, color and degree of humification

(Margalef et al., 2013). Facies A (reddish peat) is associated with very high carbon to nitrogen (C/N) ratios, low TN, low Fe and Ti values and $\delta^{13}C$ values between -21‰ and -26‰ (Figure 1). Facies B (granulated muddy peat) is a brown peat composed of coarse organic fragments, mainly roots and rootlets with low terrigenous content. High C/N ratios, low Fe and Ti content and $\delta^{13}C$ values ranging from -14‰ to -26‰ differentiate this facies (Figure 1). Facies C (organic mud) is characterized by thin layers interbedding Facies B and displaying high Fe and Ti values, high TN and relatively light $\delta^{13}C$ values (-14‰ to -22‰). Facies D (sapric peat) appears as dark and fine grains and contains organic matter with advanced degradation signs. This facies is primarily defined by high Fe and Ca content (Figure 1).

SEM analysis of Facies C sand grains revealed the presence of plagioclase and quartz grains in the coarse fraction (>500 μm). Silt particles (<50 μm) were present on Facies B and C, mainly compound of ilmenite, rutile and silica. SEM analysis of the terrigenous content of the Facies D showed that the mineral fraction below 30 μm consisted of a mixture of Al, Fe, Mn oxides and organic bounded Ca as well as other organic compounds.

4.2 Age model

A detailed description of main features of Rano Aroi age model can be found in Margalef et al. (2013). The application of mixed-effect model (Heegaard et al., 2005), instead of a linear extrapolation, introduces slight changes, preserving general patterns but improving the age determination and associated errors of the record bottom part, that lies beyond the radiocarbon limit (Figure 2).

We have restricted our study of millennial–scale variability (including stadial-interstadial oscillations) to the time window between an stratigraphic discontinuity at 38 kyr cal BP (see Margalef et al., 2013, 2014) and 65 kyr BP, therefore the MIS3/MIS4 transition (59.4 kyr BP, Svensson et al., 2008) is also included in our study (Fig. 2).

4.3 Principal Component Analysis result

Principal Component Analysis (PCA) was performed on a dataset composed of 6 variables (TN, TC, $\delta^{13}C_{res}$,Ti ,Fe and Ca) and 142 samples, which represented the aforementioned 38.5 to 65 kyr BP period (Figure 1 and 4). The first component explained 34.7% and the second component explained an additional 30.6% of the total variance (Figure 3). Ti, Fe and Ca contributed positively to the first component, whereas TN and $\delta^{13}C_{res}$ values are found at the opposite end of the first component. TN and Ti are found at the positive end of PC2 (Figure 1 and 4), whereas Ca and $\delta^{13}C_{res}$ contributed negatively to the second component. Facies C scores are related to Ti, TN and $\delta^{13}C_{res}$ variability, indicating that they are well represented by PC2 (Figures 2 and 4).

4.4 SST gradient across the equatorial Pacific

The current SST gradient between the E-W locations of the equatorial Pacific Ocean oscillates from 1.2˚C in boreal winter to 6˚C in boreal summer when the eastern equatorial upwelling system is fully developed, while the annual average SST gradient is 3.3˚C (World Ocean Data 2009; Locarnini et al., 2010). The calculated SST gradient between the western and eastern sites shows average values of 4.4˚C, with maximum values reaching 6˚C and minimum values at approximately 3˚C (Figure 4). According to their SST-calibrations the error of these SST gradients is considered to be better than ± 0.6 ºC while the discussion of this SST gradient mostly focuses on those changes which are above 1ºC or even larger (> 2ºC).

5 Discussion

5.1 Rano Aroi paleoenvironmental reconstruction

As stated in Margalef et al. (2013) and Margalef et al. (2014) three main environmental and hydrologic phases can be distinguished on the basis of the characterization of the four facies:

Open water phase represented by Facies C. During this phase, coarse sandy particles from volcanic soils were transported through dense mire vegetation and deposited at the center of this sedimentary deposit. The presence of these sandy particles would involve high precipitation rates. Low $\delta^{13}C_{res}$ isotopic values also reinforce the hypothesis that Facies C are tracking enhanced precipitation events (Margalef et al., 2014). This open water phase is tracked by high PC2 values (Figures 2 and 4) what allows us to use this component as rainfall index.

Long-term stable and near-surface water table phase evidenced by Facies A and B. This phase led the constant accumulation of peat sediments which were deposited in a *kettle hole* mire (Margalef et al., 2014), under accumulation conditions similar to the present Rano Aroi. This stable and sub-surficial water table conditions are reflected in the PC2 component by intermediate values.

A third environmental phase is represented by Facies D and can be interpreted as a result of diagenesis of previously accumulated peat (Figure 1, Margalef et al., 2013). Iron and calcium were incorporated into the mire as terrigenous particles, but affected by post-depositional remobilization with water movement and redox changes. Both chemical elements were incorporated into organic matter by complexation as Fe-Ca-humates under oxic conditions (Shotyk et al., 1996, Margalef et al., 2014).

5.2 Precipitation patterns over the tropical and subtropical Pacific during MIS 3

The occurrence of 6 wet events - labeled Ar1 to Ar6- have been identified between 38.5 and 65 kyr BP based on their high PC2 values (Figure 1). Three of these wet periods (Ar2, Ar4 and Ar6) are particularly outstanding. These periods are characterized by an abrupt onset and last for approximately 2,000 years. The other three wet events (Ar1, Ar3 and Ar5) are also characterized by an abrupt start but are of minor intensity and duration, lasting approximately 1,000 years or less (Figure 4 and 6). A comparison of the PC2 scores of the Rano Aroi record with other well-established climate records from the Northern and Southern Hemispheres indicates that the three major Rano Aroi events can tentatively be correlated with the North Atlantic HS 5 (ca. 47 kyr BP), 5a (ca. 53 kyr BP) and 6 (ca. 60 kyr BP), whereas the three minor events can be correlated with other DO stadials (Figures 5 and 6). Ar1, Ar2 and Ar3 wet events are located within the part of the age model well-constrained by radiocarbon dating and show a good correlation with DO stadials and Heinrich events. This pattern is maintained in the bottommost part of the record, therefore supporting the Rano Aroi chronological framework (Figure 4 and 6).

The link between the Rano Aroi wet events and the DO stadials is that is mechanistically coherent with the regional atmospheric and oceanographic reconstructions from independent proxy records. Some of the most solid evidence of atmospheric teleconnections for the DO oscillations come from Northern Hemisphere records such as speleothem records from the Hulu cave speleothems in China (Wang et al., 2001), the reflectance record from the Cariaco basin, northern Venezuela (Peterson et al., 2000; Haug et al., 2001) and changes in surface salinity in the Sulu sea indicated by core MD 97-2141 (Oppo et al., 2003; Dannenmann et al., 2003; Rosenthal et al., 2000). All of these records consistently indicate the dominance of dry conditions during the HS and other DO stadials (Table 1, Figure 5). These events have been associated with the opposite behavior in the Southern Hemisphere, as documented by wet events recorded in Northern Brazil travertine formations (Wang et al., 2007) and in marine cores offshore of the South American Atlantic coast (Arz et al., 1998), which correlate with the Rano Aroi major wet events (Figure 5). A similar climatic pattern has been described by Muller et al. (2008b) in the Lynch crater (Table 1) peat record in North Australia over the last 45 kyr cal BP. This tropical asynchrony between the two hemispheres has been explained by latitudinal migrations of ITCZ (Peterson et al., 2000; Tierney et al., 2008; Leduc et al., 2009). Changes in the AMOC and atmospheric coupling during DO stadials (interstadials) seems to provoke the southward (northward) displacement of ITCZ (Zhang and Delworth, 2005, Clement and Peterson, 2008, Chiang and Bitz, 2005; Timmermann et al., 2005). Other authors propose that main changes in ITCZ migration and in SST temperatures of tropical Pacific were also linked to monsoon fluctuations. For example, Oppo and Sun (2005) suggested the connection between periods of reduced precipitation due to a weaker monsoon over South China Sea during HS.

Although several studies support the occurrence of these ITCZ migrations, changes in the position of the SPCZ low-pressure belt are less well known. In spite of both structures are intimately related, precipitation over Easter Island is primarily determined by the arrival of cyclogenic storms generated on the SPCZ (Junk and Claussen, 2011). Easter Island hydrologic changes might record then, millennial-scale oscillations in the expansion of the SPCZ, coupled with ITCZ migrations. This could be explained by an eastward expansion of the SPCZ associated to the southwards shift in the ITCZ during MIS 3, in a Pacific configuration resembling the austral summer. However, stronger efforts on finding records capable to track SPCZ activity during MIS 3 and modeling support are required to completely understand MIS 3 Central Pacific configuration. Rano Aroi record suggests that abrupt hydrological oscillations were present not only during HS but also during other shorter DO stadials (Figure 5). Rano Aroi record also shows how hydrological conditions underwent abrupt changes meaning a rapid response to AMOC. These abrupt shifts differed from the Southern Hemisphere thermal response, which involved gradual onsets and terminations, as seen in Antarctic ice core records (Schmittner et al., 2003; Blunier et al., 1998; Blunier and Brooks, 2001; EPICA, 2006) (Figure 5).

5.3 Changes in the E-W Equatorial SST gradient of the Pacific Ocean during MIS 3

Some climate models propose that North Atlantic cold events eventually lead to changes in the Walker circulation (Zhang and Delworth, 2005). Following Zhang and Delworth (2005) modeling, the southeastern trade winds were weakened during North Atlantic melting events, and, consequently, the upwelling in the eastern equatorial Pacific was drastically reduced what could be related to ITCZ migration and to ENSO-state changes. This hypothesis can be tested by examining a reconstruction of the SST gradient across the equatorial Pacific using the temperature differences between the eastern cold tongue and the western warm pool. Low values in the SST gradient would be consistent with a weakening of the Walker circulation and should reflect periods of diminished upwelling activity in the eastern equatorial Pacific. Eastern Pacific upwelling is responsible for the upward transport of relatively cold and salty waters, whereas the very warm and fresh waters are dominant in the western Pacific warm pool (Kessler, 2006). By contrast, higher SST gradient values should be consistent with intensified upwelling in the eastern equatorial Pacific, whereas a reduced gradient indicates more homogenous hydrographic conditions along the Equator.

The obtained gradient present lower values of zonal SST gradient coincident with the Rano Aroi wet events (Figure 4). Consequently, the lower equatorial SST gradient associated to DO stadials is consistent with a muted upwelling in the eastern Equatorial Pacific and a weaker Walker circulation, which ultimately would favors a southward shift in the ITCZ and an eastward expansion of the SPCZ, as is interpreted from the Rano Aroi record. This configuration would be in line with the already proposed ENSO-like state during cold North Atlantic periods and the southward migration of the ITCZ based in climate models (Clement and Cane, 1999) and also in proxy reconstructions (Haug et al., 2000; Fedorov and Philander; 2000, Koutavas et al., 2006; Zuraida et al., 2009; Bolliet et al., 2011). An analogous correlation can be described based on present day instrumental data: extreme El Niño events are characterized by a mean southward migration of the Pacific ITCZ (Haug et al., 2000; Fedorov and Philander; 2000) and by an eastward and northward migration of the SPCZ (Vincent et al., 2009).

Nevertheless, other models consider these atmospheric mechanisms less relevant and instead highlight the role of the ocean's circulation through a global baroclinic adjustment when the North Atlantic cools and when there is a reduction in the AMOC. These models suggest that North Atlantic water density variations can lead to changes in the global thermocline within a few years to decades (Huang et al., 2000). These authors describe changes in the Pacific thermocline and argue that, despite the occurrence of climatic fluctuations that can be explained without invoking a link between El Niño and stadials, the existence of such a linkage cannot be excluded (Huang et al., 2000, Timmermann et al., 2005).

5.4 Southern Hemisphere tele-connections: from tropical to high latitudes

The southward migration of the ITCZ results in both a reinforcement of the equator-to-pole pressure gradient over the Southern Hemisphere and in an intensification of the Southern Westerlies (SW) (Toggweiler et al., 2006; Anderson and Carr, 2010; Heirman, 2011; Pichat et al., 2014). Changes in the position and intensity of the SW during MIS 3 should have promoted storminess over Central Pacific and contributed to an eastward movement of storms generated under the SPCZ. Another process intimately linked with the SW is the formation of intermediate water masses in the Southern Ocean. Changes in the formation rate of Antarctic Intermediate Water (AAIW) associated with DO cycles have been described in a marine record from Chatman Rise, East New Zealand (MD97-2120, 45º32.06' S, 174º55.85' E, Pahnke and Zahn, 2005) on the basis of the benthic foraminiferal $\delta^{13}C$ record (Figures 5 and 6). It has been demonstrated that periods of increased AAIW production were in phase with Southern Hemisphere warming and southward shifts of the ITCZ (Pahnke and Zahn, 2005). During DO stadials, the Antarctic continent and Southern Ocean warmed as a result of the bipolar seesaw, and, consequently, Antarctic sea ice retreated (Anderson and Carr, 2010; Skinner et al., 2010). This reduced sea ice extent would contribute to enhanced upwelling of circumpolar deep water and to a more efficient downwelling of AAIW (Toggweiler et al., 2006; Anderson and Carr, 2010; Skinner et al., 2010) (Figure 5). A recent study using Nd isotopes as a proxy for water mass provenance demonstrated that an increased export of AAIW from the Southern Ocean to tropical regions occurred during Northern Hemisphere cold periods such as HS (Pena et al, 2013). This oceanic circulation scenario also induced the release of oceanic CO_2, which was stored in poorly ventilated deep-water masses, to the atmosphere (Anderson and Carr, 2010; Skinner et al., 2010). In the context of the Rano Aroi wet events, these specific oceanic conditions in the Southern Ocean during DO stadials could have cause increased precipitation over Central Pacific.

6 Conclusions

The Rano Aroi peat record provides a unique opportunity to understand the evolution of South Pacific climate during the late Pleistocene. This record contains information concerning climate variability during MIS 3 and is located thousands of kilometers away from other continental and marine paleoclimatic records..

Anti-phase changes in precipitation and hydrology have been observed in low-latitude areas of the Northern and Southern Hemispheres. These changes have already been linked to North Atlantic cold stadials through a southward displacement of the ITCZ, as described by several studies based on both numerical climate models and environmental reconstructions from Circum-Pacific sites. The Rano Aroi record allowed us to propose that these stadials were also associated with an eastward expansion of the SPCZ, highlighting a close coupling between the migration of the ITCZ and potentially the SPCZ on millennial timescales. Future studies on past climate modeling are required to fully understand the behavior and interaction between ITCZ and SPCZ during the Late Pleistocene. The abrupt character of the Rano Aroi humid events demonstrates the rapid atmospheric response of the tropical regions to the DO-related sudden changes in the AMOC, in contrast to the more progressive heat redistribution in the Southern Ocean led by the bipolar seesaw. The Rano Aroi wet events have been correlated with periods of a reduced SST gradient along the Equator, suggesting that more humid conditions over the Easter Island region occurred when the Walker circulation was reduced. These atmosphere-ocean connections in the tropical Pacific could be considered analogous to modern El Niño- like conditions. Associated changes in the Southern Ocean with strengthened Southern Westerlies, enhanced AAIW production and sea ice retreat during DO stadials, could have also reinforced the SPCZ extension over Easter Island.

Acknowledgements

This research was funded by the Spanish Ministry of Science and Education through the projects LAVOLTER (CGL2004-00683/BTE), GEOBILA (CGL2007-60932/BTE), PALEONAO (CGL2010-15767) and RAPIDNAO (CGL2013-40608R) and through undergraduate CSIC JAE-Pre grant (BOE 04/03/2008) to Olga Margalef. We would like to thank Hans Joosten, Alex Barthemles, John Couwenberg, Martin Theuerkauf, Susanne Abel, Almut Spangenberg, Dirk Michaelis and René Dommain for their help and contributions to the peatland characterisation during O.M.'s stay at the University of Greifswald.

References

Andersson, A., Bakan, S., Fennig, K., Grassl, H., Klepp, C.-P., and Schulz, J.: Hamburg Ocean Atmosphere Parameters and Fluxes from Satellite Data – HOAPS-3 – monthly mean, World Data Center for Climate, 3097, 385-393, 2007.

Anderson, R. F., Carr, M. E.: Uncorking the Southern Ocean's Vintage CO2. Science, 328, 1117-1118, 2010.

Arz, H. W., Pätzold, J., Wefer, G.: Correlated millennial-scale changes in surface hydrography and terrigenous sediment yield inferred from last-glacial marine deposits off Northeastern Brazil. Quaternary Research 50, 157 -166, 1998.

Aucour, A.-M., Bonnefille, R.,Hillaire-Marcel, C.: Sources and accumulation rates of organic carbon in an equatorial peat bog (Burundi, East Africa) during the Holocene: carbon isotope constraints. Paleogeography, Paleoclimatology, Paleoecology 150, 179–189, 1999.

Azizi, G., Flenley, J.R.: The last glacial maximum climatic conditions on Easter Island. Quaternary International 184, 166–176, 2008.

Baker, P. A., Rigsby, C. A., Seltzer, G. O. , Fritz, S. C., Lowenstein, T. K. , Bacher, N. P., Veliz, C.: Tropical climate changes at millennial and orbital timescales on the Bolivian Altiplano, Nature, 409, 698–700, 2001.

Baker, P.A., Rigsby, C.A., Seltzer, G.O., Fritz, S.C., Lowenstein, T.K., Bacher, N.P., Veliz, C.: Tropical climate changes at millennial and orbital time scales on the Bolivian Altiplano. Nature 409, 698– 701, 2001.

Blaauw, M.: Methods and code for 'classical' age-modelling of radiocarbon sequences, Quaternary Geochronology, Volume 5, Issue 5, Pages 512–518, 2010.

Blunier, T., Brook, E.J.: Timing of millennial-scale climate change in Antarctica and Greenland during the last glacial period. Science 291, 109–112, 2001.

Blunier, T., Chappellaz, J., SchwanderJ., Dällenbach,, A., Stauffer, B., Stocker, T. F., Raynaud, D., Jouzel, J., Clausen, H. B., Hammer, C. U., Johnsen, S. J.: Asynchrony of Antarctic and Greenland climate change during the last glacial period. Nature 394, 739, 1998.

Bolliet, T., Holbourn, A., Kuhnt, W., Laj, C., Kissel, C., Beaufort, L., Kienast, M., Andersen, N., Garbe-Schönberg, D., 2011. Mindanao Dome variability over the last 160 kyr: Episodic glacial cooling of the West Pacific Warm Pool, 1994.

Broccoli, A. J., Dahl, K. A. and Stouffer. R. J.: Response of the ITCZ to Northern Hemisphere cooling, Geophysical Research Letters, 33, 1-4, 2006.

Broecker, W.: Massive iceberg discharges as triggers for global climate change. Nature 372, 421-424, 1994.

Butler, K., Prior, C.A., Flenley, J.R.: Anomalous radiocarbon dates from Easter Island. Radiocarbon 46, 395–405, 2004.

Taylor, C., Yang, Q., Zielinski, G. A.: Preliminary depth-age scale of the GISP2 ice core, Special CRREL Report, 94-1 (US), U. S. Army Corps of Eng., Hanover, N.H., 1994.

Cañellas-Boltà, N., Rull, V., Sáez, A., Margalef, O., Giralt, S., Pueyo, J.J., Birks, H.H., Birks, H. J. B., Pla-Rabes, S.: Macrofossils in Raraku Lake (Easter Island) integrated with sedimentary and geochemical records: towards a paleoecological synthesis. Quaternary Science Reviews 34: 113-126, 2013.

Cañellas-Boltà N, Rull V, Sáez A, Margalef O, Bao R, Pla-Rabes S, Blaauw M, Valero-Garcés B, Giralt S. Vegetation changes and human settlement of Easter Island during the last millennia: a multiproxy study of the Lake Raraku sediments. Quaternary Science Reviews 72: 36-48, 2013.

Chiang, J. C. H., and Bitz, C. M.: Influence of high latitude ice cover on the marine Intertropical Convergence Zone, Clim. Dyn., 25, 477–496, doi:10.1007/s00382-005-0040-5, 2005.

Clement, A.C., Peterson, L.C.: Mechanisms of abrupt climate change of the last glacial period. Reviews of Geophysics 46, 2008.

Conroy, J.L.; Overpeck, J. T.; Cole, J. E.; Shanahan, T. M.; Steinitz-Kannan, M.: Holocene changes in eastern tropical Pacific climate inferred from a Galápagos lake sediment record. Quaternary Science Reviews, 27, 1166-1180, 2008.

Cruz Jr, F. W., Burns, S. J., Kamman, I., Sharp, W. D., Vuille, M., Cardoso, A. O., Ferrari, J. A., Silva Dias, P. L., Viana Jr., O.: Insolation-driven changes in atmopsheric circulation over the past 116000 years in subtropical Brazil. Nature, Vol. 434, 63-66, 2005.

Damman A. W. H., Tolonen, K., Salanus, T.: Element retention and removal in the ombrotrophic peat of Hadekeias, a boreal Finnish peat bog, Suo 43, 137-145, 1992.

Dannenmann, S., B. K. Linsley, D.W. Oppo, Y. Rosenthal, and L. Beaufort,: East Asian Monsoon Forcing of Suborbital variability in the Sulu Sea during Marine Isotope Stage 3: Link to Northern Hemisphere Climate. Geochemistry, Geophysics, Geosystems, 4, issue 1, 1-13, 2003.

Dansgaard, W., S. J. Johnsen, S. J., Clausen, H. B., Dahl-Jensen, D., Gundestrup, N. S., Hammer, C. U., Hvidberg, C. S., Steffensen, J. P., Sveinbjörnsdottir, A. E., Jouzel, J., Bond, G.: Evidence for general instability of past climate from a 250-kyr ice core record. Nature, 364, 218–220, 1993.

Danzeglocke, U., Jöris, O., Weninger, B.: CalPal-2007 online. http://www.calpal-online.de/ accessed 2009.05.03, 2008.

Dong, B.-W., and Sutton, R. T.: Adjustment of the coupled ocean–atmosphere system to a sudden change in the thermohaline circulation, Geophys. Res. Lett., 29(15), 2002.

Dumont, H.J., Cocquyt, C., Fontugne, M., Arnold, M., Reyss, J.-L., Bloemendal, J., Oldfield, F., Steenbergen, C.L.M., Korthals, H.J., Zeeb, B.A.: The end of moai quarrying and its effect on Rano Raraku, Easter Island. Journal of Paleolimnology 20, 409–422, 1998.

EPICA Community Members,: One-to-one coupling of glacial climate variability in Greenland and Antarctica. Nature 444, 195-198¸2006.

Fedorov, A. V., Philander S. G.: Is El Niño Changing? Science 288. 1997-2002, 2000.

Flenley, J.R., King, S.M.: Late Quaternary pollen records from Easter Island. Nature 307, 47–50, 1984.

Flenley, J.R., King, S.M., Jackson, J., Chew, C., Teller, J.T., Prentice, M.E: The Late Quaternary vegetational and climatic history of Easter Island. Journal of Quaternary Science 6, 85–115, 1991.

Ganopolski, A., Rahmstorf, S., Abrupt Glacial Climate Changes due to Stochastic Resonance. Physical review letters, Volume 88, Number 3, 2002.

Genz, J., Hunt, T.L.: El Niño Southern Oscillation and Rapa Nui prehistory. Rapa Nui Journal 17 (1), 7–14, 2003.

Gossen, C.:report: The mistery lies in the Scirpus. Rapa Nui Journal 21 (2), 105-110, 2007.

Grootes, P. M., Stuiver, M., White, J. W. C., Johnson, S., Jouzel, J.: Comparison of oxygen isotope records from the GISP2 and GRIP Greenland ice cores. Nature 366, 552–554, 1993.

Haug, G.H., Hughen, K. A., Sigman, D.M., Peterson, L. C., Röhl, U.: Southward Migration of the intertropical convergence Zone through the Holocene. Science 293, 1304-1308, 2005.

Heegaard, E., Birks, H. J. B., Telford, R. J.: Relationships between calibrated ages and depth in stratigraphical sequences: an estimation procedure by mixed-effect regression. The Holocene, 15, 4; pp 612-618, 2005.

Heinrich, H.: Origin and consequence of cyclic ice rafting in the northeast Atlantic Ocean during the past 130000 years, Quat. Res., 29, 142–152, 1988.

Heirman, K.: “A wind of Change”. Changes in position and intesity of the Southern Hemisphere Westerlies during Oxygen Isotope Stages 3, 2 and 1. PhD Thesis. University of Gent, 2011.

Hemming, S. R.: Heinrich events: Massive late pleistocene detritus layers of the North Atlantic and their global climate imprint. *Rev. Geoph.*42, RG1005, 2004.

Herrera, C., Custodio, E.: Conceptual hydrogeological model of volcanic Easter Island (Chile) after chemical and isotopic surveys. Hydrogeology Journal. 16, 1329-1348, 2008.

Hong, Y.T., Wang, Z.G., Jiang, H.B., Lin, Q.H., Hong, B., Zhu, Y.X., Wang, Y., Xu, L.S., Leng, X.T., Li, H.D.: A 6000-year record of changes in drought and precipitation in northeastern China based on a 13C time series from peat cellulose, Earth Planet. Sci. Lett. 185, 111–119, 2008.

Horrocks, M., Wozniak, J.A. Plant microfossil analysis reveals disturbed forest and mixed-crop, dryland production system at Te Niu, Easter Island. Journal of Archaeological Science 35, 126–142, 2008.

Huang, R. X., Cane, M. A., Naik, N., Goodman, P.: Global adjustment of the thermocline in response to deepwater formation, Geophys. Res. Lett., 27, 759 – 762, 2000.

Joosten, H., Clarke, D.: Wise Use of Mires and Peatlands - Background Principles including a Framework for Decision-Making. International Mire Conservation Group and International Peat Society, Saarijärvi, Finland, 2002.

Junk, C., Claussen, M.: Simulated climate variability in the región of Rapa Nui during the last millenium. Climate of the Past 7, 579-586, 2011.

Kessler, W. S.: The circulation of the eastern tropical Pacific: A review, Progress in Oceanography, 69, 181-217, 2006.

Koutavas, A., Menocal, P. B., Lynch-Stieglitz, J.: Holocene trends in tropical Pacific sea surface temperatures and the El Niño-Southern Oscillation. Pages, 13 (3), 22-23, 2006.

Lamy, F., Hebbeln, D., Wefer, G.: Late Quaternary precessional cycles of terrigenous sediment input off the Norte Chico, Chile (27.5S) and paleoclimatic implications. Paleogeography, Paleoclimatology, Paleoecology 141, 233-251, 1998.

Lea, D.W., Pak, D.K., Belanger, C.L., Spero, H.J., Hall, M.A., Shackleton, N.J.: Paleoclimate history of Galápagos surface waters over the last 135,000 yr. Quaternary Science Reviews 25, 1152–1167, 2006.

Leduc, G., Vidal, L., Tachikawa, K., Bard, E.: ITCZ rather than ENSO signature for abrupt climate changes across the tropical Pacific? Quaternary Research 72, 123-131, 2009.

LeGrande A.N. and Schmidt G.A.: Global gridded data set of the oxygen isotopic composition in seawater. Geophysical Research Letters 33: L12604, 2006.

Locarnini, R., Mishonov, A., Antonov, J., Boyer, T., Garcia, H., Baranova, O., Zweng, M., and Johnson, D.,: World Ocean Atlas ed. NOAA Atlas NESDIS 68, U.S. Government Printing Office, Washington, D.C, 2010.

MacIntyre, F.: ENSO, climate variability, and the Rapanui: Part I. the basics. Rapa Nui Journal 15 (1), 17–26, 2001a.

MacIntyre, F.: ENSO, climate variability, and the Rapanui: Part II. Oceanography and Rapa Nui. Rapa Nui Journal 15 (2), 83–94, 2001b.

Mann, D., Edwards, J., Chase, J., Beck, W., Reanier, R., Mass, M., Finney, B., Loret, J.: Drought, vegetation change, and human history on Rapa Nui (Isla de Pascua, Easter Island). Quaternary Research 69, 201–206, 2008.

Margalef , O. Cañellas-Boltà, N., Pla-Rabes, S., Giralt, S., Pueyo, J. J., Joosten, H., Rull, V., Buchaca, T., Hernández, A., Valero-Garcés, B. L., Moreno, A., Sáez, A.: A 70,000 year geochemical and paleoecological record of climatic and environmental change from Rano Aroi peatland (Easter Island). Global and Planetary Change, 108: 72-84, 2013.

Margalef, O.; Martínez-Cortizas, A.; Pla-Rabes, S.; Cañellas-Boltà, N.; Pueyo J. J.; Alberto Sáez, A.; Valero-Garcés, B.; Giralt, S.: Environmental processes in Rano Aroi (Easter Island) peat geochemistry forced by climate variability during the last 70 kyr. Palaeogeography, Palaeoclimatology, Palaeoecology. 414, pp. 438 – 450, 2014.

Meese, D.A., Alley, R.B., Fiacco, R.J. , Germani, M.S., Gow, A.J., Grootes, P.M. , Illing, M., Mayewski, P.A., Morrison, M.C., Ram, M., Taylor, K.C., Yang, Q., and Zielinski, G.A.: Preliminary depth-agescale of the GISP2 ice core. Special CRREL Report 94-1, US, 1994.

Meyers, P. A.: Preservation of elemental and isotopic source identification of sedimentary organic matter. Chemical Geology 114, 289-302, 1994.

Muller, J.: Reconstructing climate change of the last 55 kyr: The Lynch's Crater peat mire record, NE-QLD, Australia. PhD thesis, James Cook University, 2006.

Muller, J., Wüst, R.A.J., Weiss, D.J., Hu, Y.: Geochemical and stratigraphic evidence of environmental change at Lynch's Crater, Queensland, Australia. Global and Planetary Change 53, 269–277, 2006.

Muller, J., Kylander, M.E., Wüst, R.A., Weiss, D.J., Martinez Cortizas, A., LeGrande, N., Jennerjahn, T., Behling, H., Anderson, W. T., Jacobson, G.: Possible evidence for wet Heinrich phases in tropical NE Australia: the Lynch's Crater desposit, 2008.

Oksanen, J., Kindt, R., Legendre, P., O'Hara, RB.: vegan: Community Ecology Package. R package version 1.8-3, URL http://CRAN.R-project.org/, 2006.

Oppo, D.W., Linsley, B.K., Rosental, Y., Dannenmann, S., Beaufort, L.: Orbital and suborbital climate variability in the Sulu Sea, western tropical Pacific, Geochem. Geophys. Geosyst. 4, 20. 1-20, 2003.

Oppo, D. W., & Sun, Y.: Amplitude and timing of sea-surface temperature change in the northern South China Sea: Dynamic link to the East Asian monsoon. Geology, 33(10), 785-788, 2005.

Orliac, C., Orliac, M.: The disappearance of Easter Island's forest: overexploitation or climatic catastrophe? In: Stevenson, C., Lee, G., Morin, F.J. (Eds.) Easter Island in Pacific Context: South Seas Symposium. Proceedings of the Fourth International Conference on Easter Island and East Polynesia. Easter Island Foundation, Los Osos, pp. 129-134, 1998.

Orliac, C.: The woody vegetation of Easter Island between the early 14th and the mid-17th Centuries A.D. In: Stevenson, C., Ayres, W. (Eds.), Easter Island Archaeology: Research on Early Rapanui Culture. Easter Island Foundation, Los Osos, 2000.

Pahnke, K., Zahn, R.: Southern Hemisphere water mass conversion linked with North Atlantic Climate Variability. Science 307, 1741-1746, 2005.

Pena, L. D., Cacho, I., Ferretti, P. and Hall, M. A.: El Niño–Southern Oscillation–like variability during glacial terminations and interlatitudinal teleconnections, Paleoceanography, 23, 2008.

Pena, L. D., Goldstein, S. L., Hemming, S. R., Jones, K. M., Calvo, E., Pelejero, C. and Cacho, I.: Rapid changes in meridional advection of Southern Ocean intermediate waters to the tropical Pacific during the last 30 kyr, Earth and Planetary Science Letters, 368, 20-32, 2013.

Peteet, D., Beck,W., Ortiz, J., O'Connell, S., Kurdyla, D., Mann, D.: Rapid vegetational and sediment change from Rano Aroi crater, Easter Island. In: Loret, J., Tanacredi, J.T. (Eds.) Scientific Exploration into the World's Environmental Problems in Microcosm. Kluwer Academic/Plenum Publ., New York, pp. 81–92, 2003.

Peterson, L. C., Haug, G. H., Hughen, K. A. , and Rohl, U.: Rapid changes in the hydrologic cycle of the tropical Atlantic during the last glacial, Science 290, 1947–1951, 2000.

Pichat, S., Abouchami, W., Galer, S. J. Lead isotopes in the Eastern Equatorial Pacific record Quaternary migration of the South Westerlies. Earth and Planetary Science Letters, 388, 293-305, 2014.

R Development Core Team: R: a language and environment for statistical computing. R Foundation for Statistical Computing, Vienna, Austria. (http://www.Rproject. org/), 2011.

Reimer, P.J., Baillie, M.G.L, Bard, E., Bayliss, A., Beck, J.W., Bertrand, C.J.H, Blackwell, P.G., Buck, C.E., Burr, G.S., Cutler, K.B., Damon, P.E., Edwards, R.L., Fairbanks, R.G., Friedrich, M., Guilderson, T.P., Hogg, A.G., Hughen, K.A., Kromer, B., McCormac, G., Manning, S., Ramsey, C.B., Reimer, R.W., Remmele, S., Southon, J.R., Stuiver, M., Talamo, S., Taylor, F.W., van der Plicht, J., Weyhenmeyer, C.E.: IntCal04 terrestrial radiocarbon age calibration, 0–26 cal kyr BP. Radiocarbon 46, 1029-1058, 2004.

Rosenthal, Y., Oppo, D. W., Dannenmann, S., and Linsley, B. K.: Millennial-scale variability in western Pacific sea surface temperatures during glacial and Holocene climates, Eos Trans. AGU, 81(48), F656, Fall Meet. Suppl, 2000.

Rull, V., Cañellas-Boltà, N., Sáez, A., Giralt, S., Pla, S., Margalef, O.: Paleoecology of Easter Island: Evidence and uncertainties. Earth-Science Reviews 99, 50–60, 2010a.

Rull, V., Stansell, N. D., Montoya, E., Bezada, M., and Abbott, M. B.: Palynological signal of the Younger Dryas in tropical Venezuelan Andes. Quaternary Science Reviews 29, 3045–3056, 2010b.

Russell, J. M., Vogel, H., Konecky, B. L., Bijaksana, S., Huang, Y., Melles, M, Wattrus, M., Costa, M.., King, J. W. Glacial forcing of central Indonesian hydroclimate since 60,000 y BP. *Proceedings of the National Academy of Sciences*,*111*(14), 5100-5105, 2014.

Sáez, A., Valero-Garcés, B., Giralt, S., Moreno, A., Bao, R., Pueyo, J.J., Hernández, A., Casas, D.: Glacial to Holocene climate changes in the SE Pacific. The Raraku Lake sedimentary record (Easter Island, 27°S). Quaternary Science Reviews 28, 2743–2759, 2009.

Schmittner, A. Saenko, O.A. and Weaver, A.J: Coupling of the hemispheres in observations and simulations of glacial climate change. Quaternary Science Reviews 22: 659-671, 2003.Shotyk, W.: Peat bog archives of atmospheric metal deposition: geochemical evaluation of peat profiles, natural variations in metal concentrations, and metal enrichment factors. Environmental Reviews, 4(2): 149-183, 1996.Shotyk, W., Weiss, D., Kramers, J.D., Frei, R., Cheburkin, A.K., Gloor, M., Reese, S.: Geochemistry of the peat bog at Etang de la Gruère, Jura Mountains, Switzerland, and its record of atmospheric Pb and lithogenic trace metals (Sc, Ti, Y, Zr, and REE) since 12,370 14C yr BP. Geochimica et Cosmochimica Acta 65, 2337–2360, 2001.

Siddall, M., Rohling, E.J., Thompson, W.G., Waelbroeck, C.: Marine isotope stage 3 sea level fluctuations: data synthesis and new outlook. Rev. Geophys. 46, RG4003, 2008.

Skinner, L. C., Fallon, S., Waelbroeck, C., Michel, E., Barker, S.: Ventilation of the Deep Southern Ocean and Deglacial CO_2 rise. Science 328, 1147-1151, 2010.

Stott, L., Poulsen, C., Lund, S., Thunell, R.: Super ENSO and global climate oscillations at millennial time scales. Science 297, 222-226, 2002.

Stuut J.W., Lamy F.: Climate variability at the southern boundaries of the Namib (southwestern Africa) and Atacama (northern Chile) coastal deserts during the last 120.000 yr. Quaternary Research, 62, 301-309, 2004.

Svensson, A., Andersen, K.K., Bigler, M., Clausen, H.B., Dahl-Jensen, D., Davies, S.M., Johnsen, S.J., Muscheler, R., Parrenin, F., Rasmussen, S.O., Ro¨thlisberger, R., Seierstad, I., Steffensen, J.P., Vinther, B.M. A 60 000 year Greenland stratigraphic ice core chronology. Climate of the Past 4, 47–57, 2008.

Succow, M., Joosten, H. Landschaftsökologische Moorkunde. Stuttgart, Sweizerbart, 622p., 2001.

Tierney, J. E, Russell, J.M, Huang, Y., Sinninghe Damsté, J. S., Hopmans, E. C, Cohen, A. S.: Northern Hemisphere controls on tropical southeast African climate during the past 60.000 years. Science 322, 252-255, 2008.

Timmermann, A., Krebs, U. Justino, F., Goosse, H., and Ivanochko, T.: Mechanisms for millennial-scale global synchronization during the last glacial period, Paleoceanography, Volume 20, Issue 4, 2005.

Toggweiler, J. R., Russell, J. L., and Carson, S. R.: Midlatitude westerlies, atmospheric CO_2, and climate change during the ice ages, Paleoceanography, 21, 1-15, 2006.

Tozuka, T., T. Kagimoto, Y. Masumoto, and T. Yamagata : Simulated multiscale variations in the western tropical Pacific: The Mindanao Dome revisited, J. Phys. Oceanogr., 32(5), 1338–1359, doi:10.1175/1520-0485, 2002.

Vincent, E., Lengaigne, M., Menkes, C. E., Jourdain, N. C., Marchesiello, P., Madec, G.: Interannual vairiability of the South Pacific Convergence Zone and implications for tropical cyclone genesis. Clim Dyn. 36, 1881-1896, 2009.

Wang, X., Auler, A. S., Edwards, R. L., Cheng, H., Cristalli, P. S., Smart, P. L., Richards, D. A., and Shen, C.-C.: Wet periods in northeastern Brazil over the past 210 kyr linked to distant climate anomalies. Nature 432, 740 – 743, 2004.

Wang, X., Auler, A. S., Edwards, R. L., Cheng, H., Ito, E., Wang, Y., Kong, X., Solheid, M.: Millennial-scale precipitation changes in southern Brazil over the past 90,000 years, Geophysical Research Letters, Vol. 34, 1-5; 2007.

Weninger, B., Jöris, O., Danzeglocke, U.: CalPal-2007. Cologne Radiocarbon Calibration & Paleoclimate Research Package, 2008.

Weiss, D., Shotyk, W., Rieley, J.O., Page, S.E., Gloor, M., Reese, S., Cortizas-Martínez, A.: The geochemistry of major and selected trace elements in a forested peat bog, Kalimantan, SE Asia, and its implications for past atmospheric dust deposition. Geochimica et Cosmochimica Acta 66, 2307–2323, 2002.

Xie, S.P.: On the genesis of the equatorial annual cycle, J. Clim., 7, 2008 – 2013, 1994.

Yuan, X.: ENSO-related impacts on Antarctic sea ice: A synthesis of phenomenon and mechanisms. Antarct. Sci., 16, 415–425, doi:10.1017/S0954102004002238, 2004.

Zhang, R., Delworth, L. T.: Simulated Tropical Response to a Substantial Weakening of the Atlantic Thermohaline Circulation. American Meterorological Society 18. 1853-1860, 2005.

Zuraida, R., Holbourn, A., Nürnberg, D., Kuhnt, W., Dürkop, A., & Erichsen, A.: Evidence for Indonesian Throughflow slowdown during Heinrich events 3–5. Paleoceanography, *24*(2), 2009.

Tables

Name	Site	Latitude	Longitude	Age (kyr BP)	Reference
TERRESTRIAL	**RECORDS**				
Hulu Cave	Southern China	32°30’N	119°10'E	75	Wang et al., 2001
Lynch's Crater	Northeast Australia	17°37'S	145°17' E	45	Muller et al., 2008b
Rano Aroi*	**Easter Island**	**27°07’S**	**109°22’W**	**70**	**Margalef et al., 2013; Margalef et al., 2014**
Botuverá cave	Northeastern Brazil caves	27°13' S	49°09' W	90	Wang et al., 2007
TERRESTRIAL	**RECORDS**				
ODP 1145	South China Sea	19°35' N	117°38' E	145	Oppo and Sun., 2005
MD 01-2378	Sulu Sea (Indic Ocean)	13°05'N	121°47'E	62	Zuraida et al., 2009
ODP 1002	Cariaco Basin (Atlantinc Ocean)	10°43’N	65° 10' W	90	Peterson et al., 2000; Haug et al., 2001
MD 97-2141	Sulu Sea	8.8°N	121.3°1 E	400	Oppo et al., 2003; Dannenmann et al., 2003; Rosenthal et al., 2000
MD 06-3067	West Equatorial Pacific Ocean	6°31'N	126°30'W	160	Bolliet et al., 2011
ODP 1240	Panama Basin (Pacific Ocean)	0° 01'N	86°28' E	275	Pena et al., 2008
GeoN 3104	Fortaleza (Atlantic Ocean)	3°40’S	37°43W	85	Arz et al., 1998
GeoB 3375	Northen Chile (Pacific Ocean)	27° 28'S	71° 15'W	120	Stuut and Lamy, 2004
MD97-2120	Chatham Rise (Southern Ocean)	45°32'S	174°56'E	340	Pahnke and Zahn, 2005
ICE RECORDS					
GISP	Greenland	72° 35' N	37° 45' W	90	Blunier et al., 2001
Byrd	West Antarctic	80° S	119°30'W	90	Blunier et al., 2001

Table 1. Location and age extension of main records mentioned in the text and in Figures 5 and 6.

Figure captions

Figure 1. Geochemical proxies analyzed in ARO 06 01 core versus depth. Peat facies and radiocarbon ages are indicated in the first column. Geochemical proxies: TC, TN, (in percentages), C/N ratio, and $\delta^{13}C$ (‰) is indicative of the origin of organic matter. Residual values of $\delta^{13}C_{res}$ (‰) are used to enhance the presence of $\delta^{13}C$ dips. Fe, Ti and Ca FRX measurements (in cps) and Fe/Ti, Ca/Ti ratios are also shown together with the scores of PC2.

Figure 2. Rano Aroi age model. Samples from ARO 06 01. Ages in red were rejected by reflecting inversions (Margalef et al., 2013). Ages in grey lied beyond radiocarbon limit. Error bars for each point are shown. Black lines show the result of the mixed-effect model performed between 235 and 750 cm depth and extrapolated until the bottommost part of the record. Green dashed lines are showing the confidence limits.

Figure 3. Principal component analysis of the geochemical data ($\delta^{13}C_{res}$ Ti, Fe, Ca, TN, TC and C/N). Two principal component axes explain more than 60% of the variability (Axis 1: 34.7%, Axis 2: 30.6%). Variable loadings and sample scores are presented in the plane defined by the first two axes. Wet events are associated with high Ti and TN and with low $\delta^{13}C_{res}$, which are representative of flood conditions.

Figure 4. Comparison between Rano Aroi PC2 humidity index (green line) and W-E temperature (ºC) gradient over the Equatorial Pacific and the corresponding 5 point running average (thick black and line). The E-W gradient was obtained from the difference between MD97-2141-SST (red line, Dannenmann et al., 2003) and ODP 1240-SST (blue line, Pena et al., 2008). Wetter events in the Rano Aroi record coincide with a lower E-W temperature gradient, which implies that a displacement of the ITCZ and the SPCZ is associated with weaker oceanic circulation over the Equatorial Pacific, resembling an El Niño-like state.

Figure 5. Records of marine sediment cores from the Cariaco Basin (ODP 1002C, Peterson et al., 2000), Sulu Sea (MD97 21-41, Dannenmann et al., 2003; Oppo et al., 2003; Rosenthal et

al., 2003), South Pacific (MD97 21-20, Pahnke and Zahn, 2005) and Atlantic Caribbean (GeoB3912, GeoB3104; Arz et al., 1998); and the ice core datasets of NorthGRIP (Svensson et al., 2008) and of Byrd (Blunier and Brooks, 2001). The data presented and the correlations between each dataset have been reproduced from their original publications. North Atlantic temperature variability during DO oscillations is correlated with low-latitude millennial changes in precipitation. Northern Hemisphere records indicate the occurrence of dry periods during Heinrich stadials and other stadials and during Southern Hemisphere wet events.

Figure 6. Oceanic and atmospheric spatial patterns of millennial-scale climate change events (see discussion, section 5) that acted as climatic teleconnection mechanisms or feedbacks during MIS 3 interstadials (Map A) and HS (Map B). Black dots indicate the most relevant sites mentioned in the text, double circles indicate records also represented in Figure 5 and Rano Aroi is designated as a red star.

Figure 1

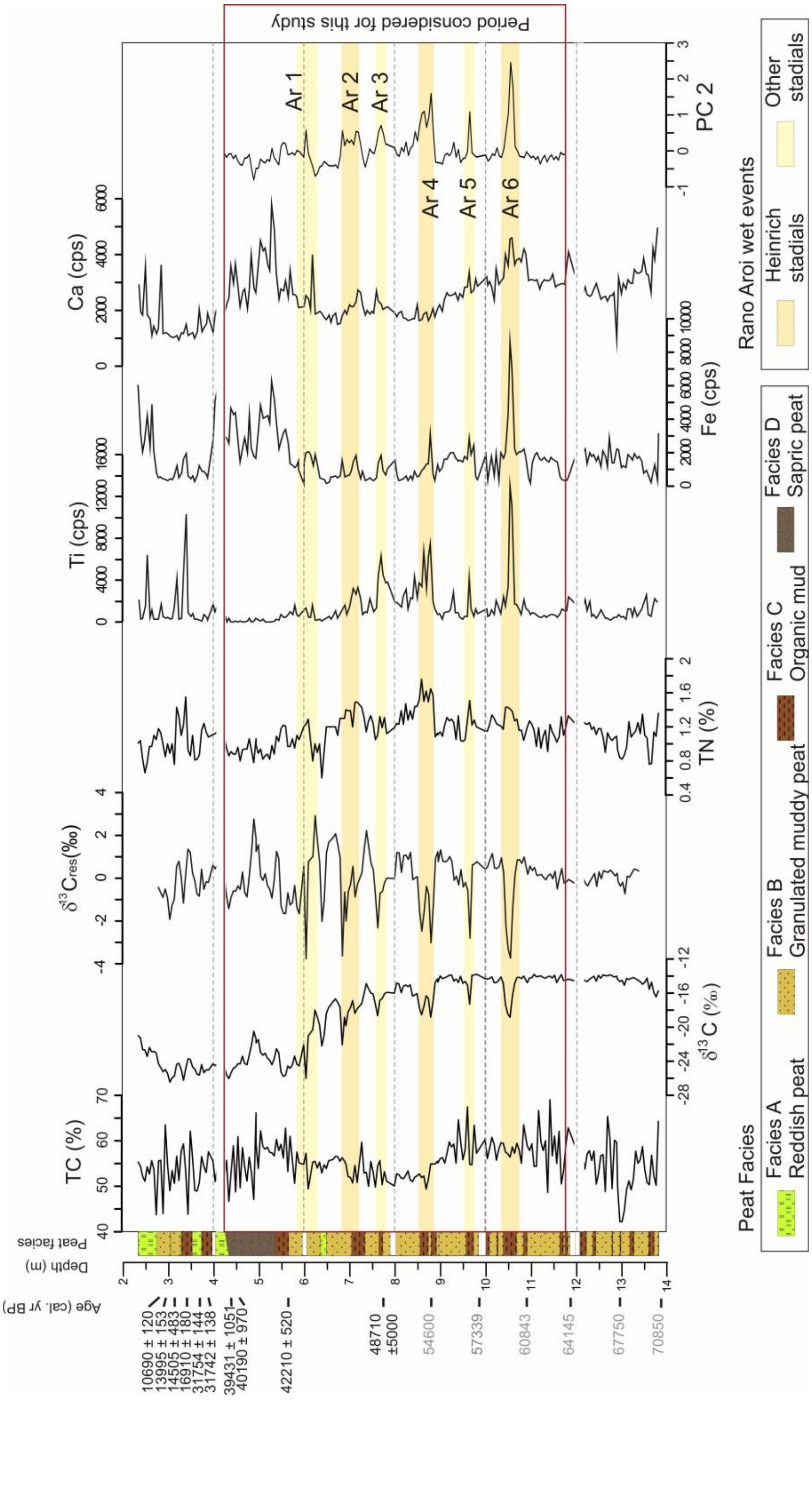

Period considered for this study
Ar 1
Ar 2
Ar 3
Ar 4
Ar 5
Ar 6
PC 2
Ca (cps)
Ti (cps)
Fe (cps)
TN (%)
δ13Cres(‰)
δ13C (‰)
TC (%)
Peat facies
Depth (m)
Age (cal. yr BP)
Rano Aroi wet events
Heinrich stadials
Other stadials
Peat Facies
Facies A Reddish peat
Facies B Granulated muddy peat
Facies C Organic mud
Facies D Sapric peat

Figure 2

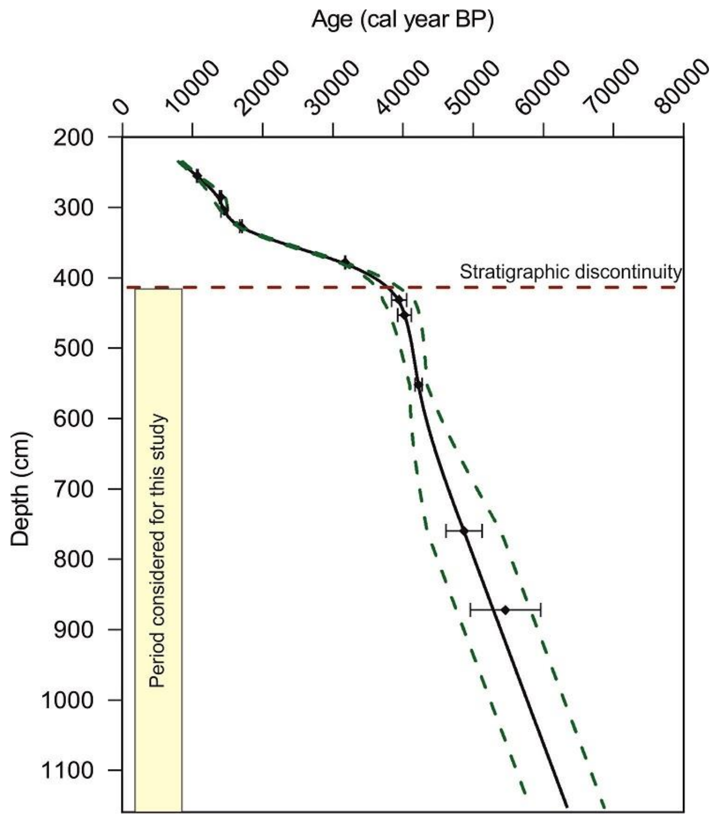
Age (cal year BP)
0
10000
20000
30000
40000
50000
60000
70000
80000
200
300
400
500
600
700
800
900
1000
1100
Depth (cm)
Stratigraphic discontinuity
Period considered for this study

Figure 3

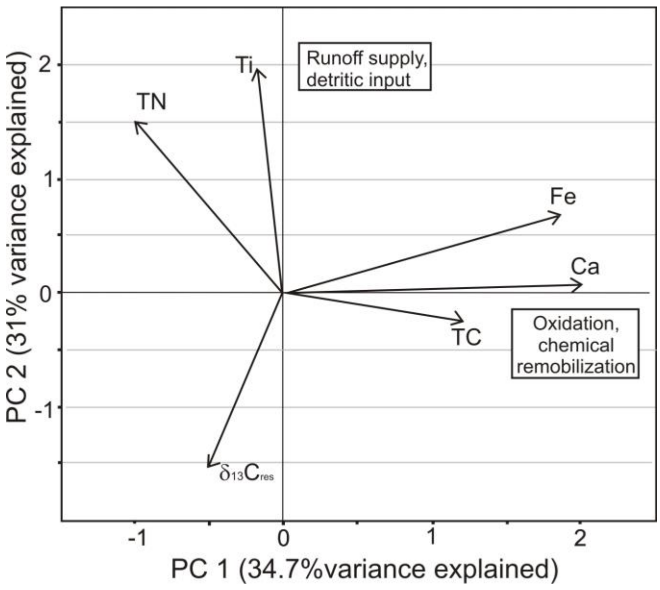

Runoff supply, detritic input
Oxidation, chemical remobilization
Ti
TN
Fe
Ca
TC
δ13Cres
PC 2 (31% variance explained)
PC 1 (34.7%variance explained)
2
1
0
-1
-1
0
1
2

Figure 4

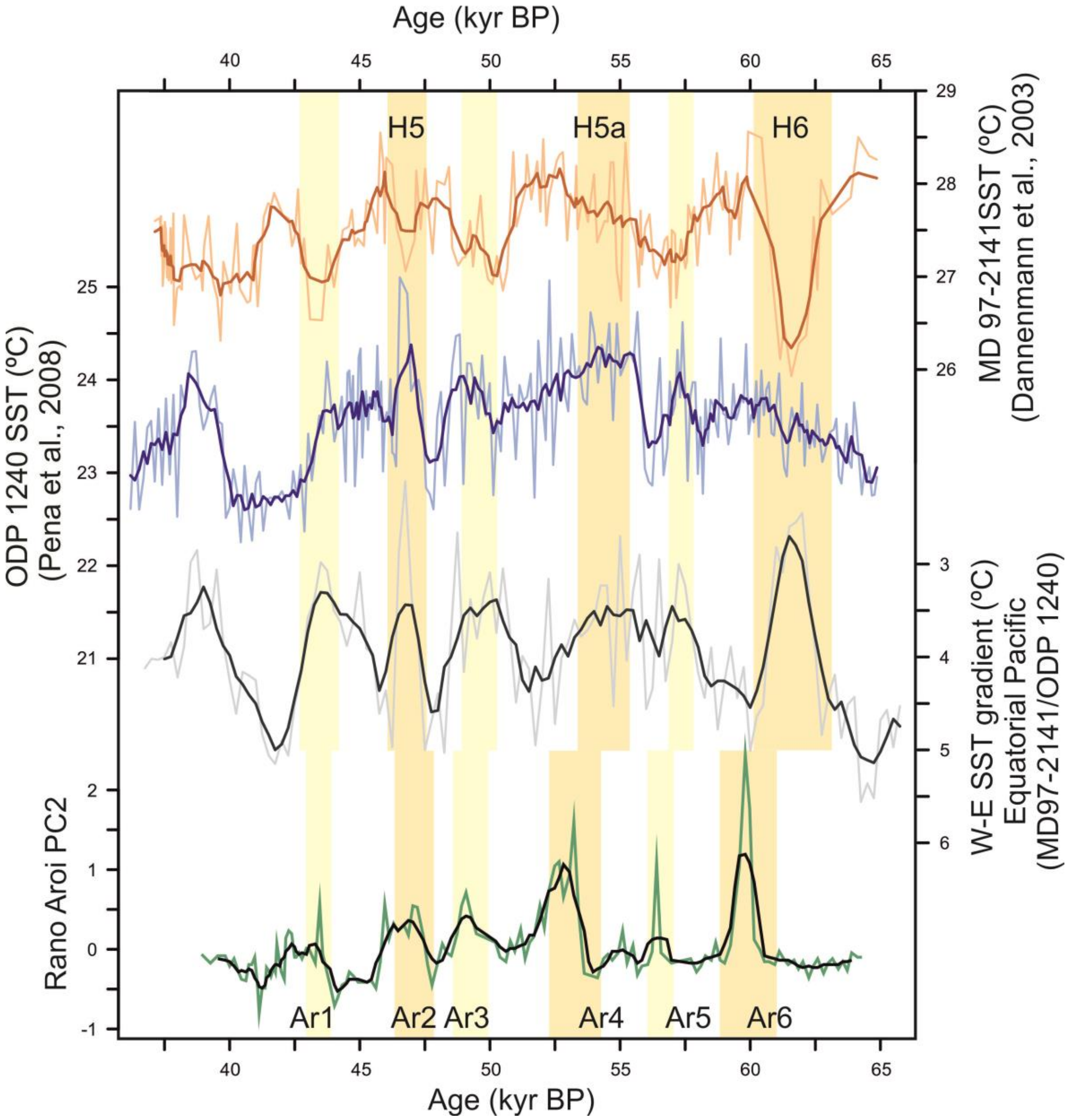
Age (kyr BP)
40
45
50
55
60
65
H5
H5a
H6
MD 97-2141SST (ºC)
(Dannenmann et al., 2003)
29
28
27
26
ODP 1240 SST (ºC)
(Pena et al., 2008)
25
24
23
22
21
W-E SST gradient (ºC)
Equatorial Pacific
(MD97-2141/ODP 1240)
3
4
5
6
Rano Aroi PC2
2
1
0
-1
Ar1
Ar2
Ar3
Ar4
Ar5
Ar6
40
45
50
55
60
65
Age (kyr BP)

Figure 5

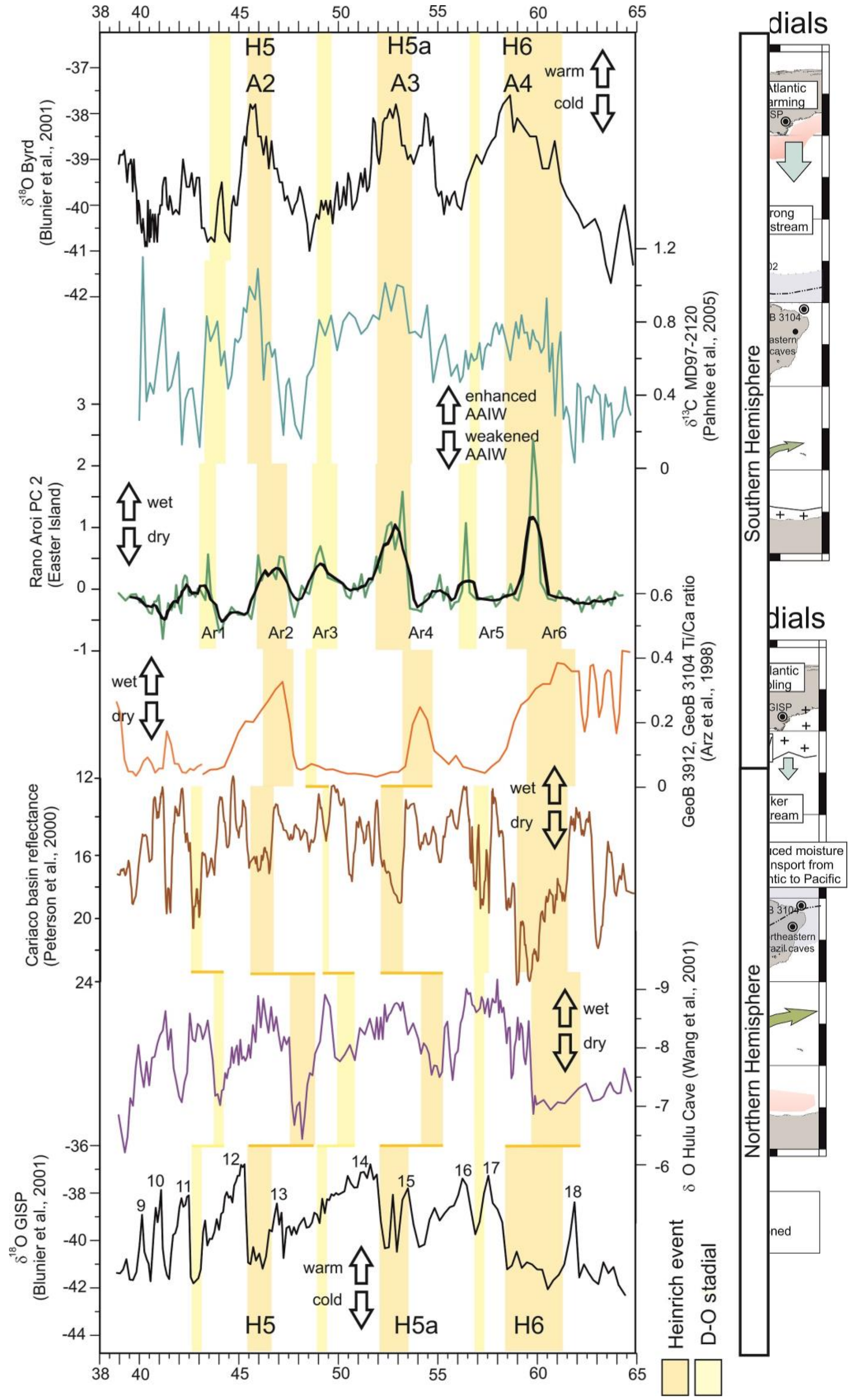

H5
A2
H5a
A3
H6
A4
warm
cold
δ18O Byrd (Blunier et al., 2001)
δ13C MD97-2120 (Pahnke et al., 2005)
enhanced AAIW
weakened AAIW
Rano Aroi PC 2 (Easter Island)
wet
dry
Ar1
Ar2
Ar3
Ar4
Ar5
Ar6
GeoB 3912, GeoB 3104 Ti/Ca ratio (Arz et al., 1998)
Cariaco basin reflectance (Peterson et al., 2000)
δ O Hulu Cave (Wang et al., 2001)
δ18O GISP (Blunier et al., 2001)
Heinrich event
D-O stadial
Southern Hemisphere
Northern Hemisphere

Additional information

Comments on Rano Aroi Age Model

Definitive ages

Part of MIS 3 lies beyond radiocarbon limit, the most widely dating technic for quaternary records. In the case of Rano Aroi mire, it was no possible to apply alternative methods because there were no tephra layers to date, nor endogenic carbonates that might allow them to be dated by U-series using laser-ablation multi-collector ICP-MS and there was no choice to use OSL techniques on sand grains because of the strong matrix effect produced by peat, rich in organic matter and water. Neither tuning methods (like $\delta^{18}O$ curves) usually performed on marine records. The solution applied to deal with this challenge and to obtain the ages for the bottommost part of the record is the use of the using a mixed-effect model and constant variance (Heegaard et al., 2005) using R software (R Development Core Team, 2011). Despite these difficulties and considering always the role of uncertainty, the reliability of our age-model can be demonstrated by the following facts:

- Peat facies and depositional system inferred in the well constrained part is the same as the bottommost part of the record and no evidences of drought episodes or discontinuities are revealed by biological and geochemical proxy (as is Facies D). Consequently, the age-depth model can be linearly expanded through time (Street-Perrott et al., 1997, Russell et al., 2014)

- The three first wet events Ar1, Ar2 and Ar3, are located within the well-constrained part of the chronological model and clearly correlate with Heinrich stadials or other. Our age model, consistently correlates the older wet events (Ar4, Ar5 and Ar 6) with North Atlantic cold stadials. The excellent time fitting between stadials and the well constrained Rano Aroi events

(<54.000 cal kyr BP) is a strong argument to postulate a correlation of the older Rano Aroi wet events (>54.000 cal kyr BP) with stadials during MIS3.

Comments on E-W equatorial gradient calculation

Several Equatorial Pacific SST reconstructions could be potentially used for the calculation of a tropical SST Pacific gradient. For this reason, we considered SST Pacific Equatorial reconstructions obtained from the same proxy (Mg/Ca ratios measured on *Globigerinoides ruber*) and depicting enough resolution between 65 and 38 kyr cal BP to resolve millennial scale variability. Accomplishing these premises, a record from eastern edge were selected (Figure 1): and ODP 1240 (Pena et al., 2008), having higher resolution than TR 163-22 (Lea et al., 2006). These two sites present slight differences on the absolute SST values (1ºC), which reflect their relative position within the cold tongue, with the warmer core (ODP 1240) located more toward the tongue edge. On the western equatorial region four published SST records were originally considered (Figure 1): MD 97-2141 (Dannenmann et al., 2003), ODP 1145 (Oppo and Sun, 2005), MD 01-2378 (Zuraida et al., 2009), and MD 06-3067 (Bolliet et al., 2011). Nevertheless, the recorded patterns were significantly different due to the complexity of the local oceanographic processes. SST variability in core MD 06-3067 is controlled by local upwelling intensity related to the Mindanao Dome activity that respond to changes in the East Asian winter Monsoon (Bolliet et al., 2011). This local SST signal during MIS 3 shows an opposite trend compared to other records of the region which respond more to atmospheric tele-connections (Bolliet et al., 2011). Core MD 01-2378 is situated under the direct influence of Indonesian throughflow, the westward current that connects the tropical Pacific with the Indian Ocean. The SST reconstruction during MIS 3 shows little changes and its evolution has been associated to thermohaline circulation but also the Australasian monsoon and sea level changes (Zuraida et al., 2009). Both core ODP 1145 located at 19°N (Oppo and Sun, 2005) and core MD97-2141 located at 10°N show SST oscillations above 1ºC during MIS 3 indicating colder conditions for HS and warmer ones for DO interstadials but the resolution of ODP 1145 record is considerably lower than the other one. For all these reasons, the SST record from core MD97-2141 has been considered the most suitable to represent regional conditions of the warm pool during MIS 3 and it has been used in our gradient calculations